

Article pubs.acs.org/est

Transformation and Mobility of Cu, Zn, and Cr in Sewage Sludge during Anaerobic Digestion with Pre- or Interstage Hydrothermal Treatment

Qian Wang, Chiqian Zhang, Haesung Jung, Pan Liu, Dhara Patel, Spyros G. Pavlostathis, and Yuanzhi Tang*



Cite This: Environ, Sci. Technol, 2021, 55, 1615-1625



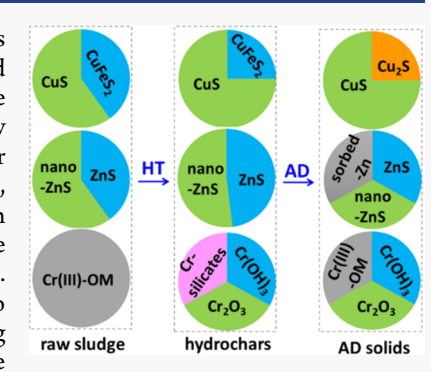
ACCESS I

Metrics & More

Article Recommendations

Supporting Information

ABSTRACT: Anaerobic digestion (AD) combined with hydrothermal treatment (HT) is an attractive technology for sewage sludge treatment and resource recovery. The fate and distribution of heavy metals in the sludge during combined HT/AD significantly affect the sludge final disposal/utilization options, yet such information is still lacking. This study systematically characterizes the transformation of important heavy metals Cu, Zn, and Cr in sewage sludge during AD with pre- or interstage HT (i.e., HT-AD or AD-HT-AD, respectively). Complementary sequential chemical extraction and X-ray absorption spectroscopy were used to characterize the speciation and mobility of metals. For the HT-AD system, both Cu and Zn predominantly occur as sulfides in HT hydrochars. Subsequent AD favors the formation of Cu₂S and partial transformation of nano-ZnS to adsorbed and organo-complexed Zn species. HT favors the formation of Cr-bearing silicates in hydrochars, whereas Fe(III)-Cr(III)-hydroxide and Cr(III)-humic complex are



the predominant Cr species in AD solids. Similar reaction pathways occur in the AD-HT-AD system with some minor differences in metal species and contents, as the first-stage AD changed the sludge matrix. These findings have important implications for understanding the fate and mobility of heavy metals in sludge-derived hydrochars and AD solids.

1. INTRODUCTION

Activated sludge process is commonly used for treating municipal wastewater at water resource recovery facilities (WRRFs). WRRFs in the US produce millions of tons of sewage sludge as a byproduct annually, among which ~55% is land applied and the remaining is disposed by landfill or incineration.2 Sewage sludge contains a wide range of contaminants, such as heavy metals, pesticides, herbicides, and pathogens,^{3,4} posing significant environmental and public health risks during land application or disposal. Thus, proper treatment before its final utilization or disposal is needed. On the other hand, sewage sludge contains high contents of organic matter, which can be converted to biomethane (renewable bioenergy) via anaerobic digestion (AD), making it a good candidate for the energy recovery. 1,5 AD consists of four key steps: hydrolysis, acidogenesis, acetogenesis, and methanogenesis.⁶ Hydrolysis, the conversion of particulate polymeric materials to bioavailable substrates for subsequent acidogenesis and acetogenesis, is the rate-controlling step of AD of particulate organic waste. Hydrothermal treatment (HT) as a prestage process for AD (i.e., sequential HT-AD) is effective in accelerating hydrolysis, increasing organic matter biodegradability, and promoting biogas (biomethane and CO₂) production during AD.⁸ Moreover, the preheated feedstock stream reduces the energy input for maintaining the subsequent AD at 35 °C.9 Recent studies have also

explored HT as an interstage process (i.e., sequential AD-HT-AD) to enhance the biodegradation of recalcitrant particulate organic matter and maximize biogas production and energy recovery. 10,11

Overall, the above discussed combined HT and AD processes (including HT-AD and AD-HT-AD, hereinafter collectively referred to as combined HT/AD) can facilitate sludge dewatering, reduce sludge volume, and improve sludge quality as a soil amendment. 12,13 Considering the important roles of heavy metals in regulations for sludge utilization and disposal, as well as the significant correlation between metal speciation, mobility, and bioavailability, an in-depth understanding of metal speciation evolution during combined HT/ AD is highly desired. Two common methods for investigating the fate of metals in solid samples are sequential chemical extraction (SCE) and X-ray absorption spectroscopy (XAS). SCE is an empirical chemical method for indirect identification of metal species. For the three-stage Community Bureau of

Received: August 3, 2020 Revised: January 1, 2021 Accepted: January 4, 2021 Published: January 19, 2021





Reference (BCR) procedure ¹⁴ used in this study, metal species are categorized to four fractions: water-/acid-soluble and exchangeable (i.e., carbonates), reducible (i.e., bound to Fe and Mn oxyhydroxides), oxidizable (i.e., bound to organic matter and sulfides), and residual fractions. ^{14,15} The metals in the acid-soluble fraction are considered to be the most mobile and readily bioavailable, whereas metals in the other fractions are considered to be relatively stable and less mobile. ¹⁶ XAS is an *in situ* and nondestructive method for obtaining direct molecular level structure information on metal speciation (e.g., oxidation state, coordination structure, and mineral phase) in heterogeneous matrices such as environmental samples. ^{15,17}

Previous studies characterizing the contents and speciation of heavy metals in sewage sludge mainly focused on AD or HT alone. The speciation of Cu and Zn in anaerobically digested sludge was dominated by sulfides based on XAS analyses. 18 However, Dong et al. reported that AD increased the bioavailability of Cu and Zn using the SCE method. 19 AD can also increase the bioavailability of Cr, a common heavy metal contaminant in sludge. 19 Similarly, HT alone can significantly affect metal speciation in sewage sludge. 15,20 Our recent study revealed that the transformation of Cu and Zn in sewage sludge during HT was highly dependent on treatment temperature. 15 Cr exists predominantly as an organo-Cr(III) complex in activated sludge, 21,22 and HT can convert bioavailable Cr fractions into more stable fractions^{23,24} as oxidizable and residual fractions in HT hydrochars.^{20,25} A recent study reported that HT under alkaline conditions favors the immobilization of Cr, while it is the opposite under acidic conditions.²⁶ To the best of our knowledge, no study has systematically investigated Cu, Zn, and Cr speciation evolution in sewage sludge during combined HT/AD. In addition, previous studies investigating Cr speciation during AD or HT alone mainly used SCE analysis, which is an empirical method that does not provide direct in situ information on the speciation of metals.^{17,2}

This study aims to (1) characterize the transformation of representative heavy metals Cu, Zn, and Cr during the combined HT/AD of sewage sludge using complementary SCE and synchrotron XAS analyses; (2) compare the effects of HT as a pre- or interstage process (i.e., HT-AD versus AD-HT-AD) on metal speciation evolution; and (3) explore the underlying mechanisms and the controlling factors such as HT temperature on metal speciation. HT was conducted at 90, 155, 125, or 185 °C to evaluate different thermal hydrolysis conditions. This study fills the knowledge gap in the speciation evolution of heavy metals during combined HT/AD of sewage sludge and provides fundamental knowledge for sustainable management of sewage sludge and other biowastes.

2. MATERIALS AND METHODS

2.1. Sludge Sample Collection. Sludge samples were collected from a municipal WRRF near Atlanta, Georgia, USA. The WRRF has primary (physical) and secondary (activated sludge) treatment units and anaerobic digesters. The sludge mixture, a blend of primary and waste activated sludges, was collected as raw sludge. Raw sludge has a total solids (TS) concentration of approximately 60 g/L. In addition, secondary wastewater effluent and anaerobic digestate were collected from the secondary clarifier and an anaerobic digester of the WRRF, respectively. The digestate was further anaerobically preincubated at 35 °C in the lab until no significant biogas production and served as the anaerobic inoculum. All samples

were stored in the dark at 4 °C before use. A portion of raw sludge was separated by centrifugation and freeze-dried for chemical composition and structure analyses as detailed below.

2.2. Combined HT/AD of Sewage Sludge. Combined HT/AD of raw sludge was conducted in the sequences of HT-AD or AD-HT-AD. The treatment conditions and sample labels are summarized in Table 1 and discussed below.

Table 1. Hydrothermal Treatment (HT) and Anaerobic Digestion (AD) Conditions and Sample Labels

system	treatment	reaction conditions and pH^a	sample label
HT- AD	raw sludge	pH 6.34	raw sludge
	AD alone	AD of raw sludge, 35 $^{\circ}$ C, 79 days, and pH 7.69	A79
	HT alone	90 °C, 4 h, and pH 6.04	H90
	HT-AD	AD of H90-derived slurries, 35 °C, 79 days, and pH 7.49	H90A
	HT alone	155 °C, 4 h, and pH 5.67	H155
	HT-AD	AD of H155-derived slurries, 35 °C, 79 days, and pH 7.47	H155A
	HT alone	185 °C, 4 h, and pH 5.41	H185
	HT-AD	AD of H185-derived slurries, 35 °C, 79 days, and pH 7.46	H185A
		77 (2)	
AD- HT- AD	raw sludge	pH 6.34	raw sludge
	AD alone	AD of raw sludge, 35 $^{\circ}$ C, 15 days, and pH 7.60	A15
	AD-AD	AD of A15-derived slurries, 35 °C, 74 days (89 days in total), and pH 8.44	A89
	AD-HT	HT of A15 solids, 90 $^{\circ}$ C, 4 h, and pH 7.53	AH90
	AD-HT- AD	AD of AH90-derived slurries, 35 °C, 74 days, and pH 8.45	AH90A
	AD-HT	HT of A15 solids, 125 $^{\circ}$ C, 4 h, and pH 7.26	AH125
	AD-HT- AD	AD of AH125-derived slurries, 35 °C, 74 days, and pH 8.38	AH125A
	AD-HT	HT of A15 solids, 155 $^{\circ}$ C, 4 h, and pH 7.24	AH155
	AD-HT- AD	AD of AH155-derived slurries, 35 °C, 74 days, and pH 8.37	AH155A
	AD-HT	HT of A15 solids, 185 °C, 4 h, and pH 6.91	AH185
	AD-HT AD-HT- AD		AH185 AH185A

2.2.1. HT-AD System. HT of raw sludge (130 mL per reactor) was performed using 200 mL polypropylene-lined stainless-steel hydrothermal reactors (COL-INT TECH, SC, USA). The reactors were tightly sealed and heated in an oven at 90, 155, or 185 °C for 4 h (3 h ramping and 1 h holding time at the target temperature; six replicates) and then naturally cooled down to room temperature. A portion of the HT-treated sludge (HT-derived slurry hereinafter) was separated by centrifugation into solids (hydrochars hereinafter, although HT at 90 °C did not readily convert biomass to chars) and supernatants (HT process water hereinafter). The hydrochars were freeze-dried and used for composition and structure analyses.

HT-derived slurry that was not separated was transferred to 600 mL glass AD reactors to achieve a final concentration of 2 g volatile solids (VS)/L. The total sludge suspension volume was 400 mL in each AD reactor, which also contained

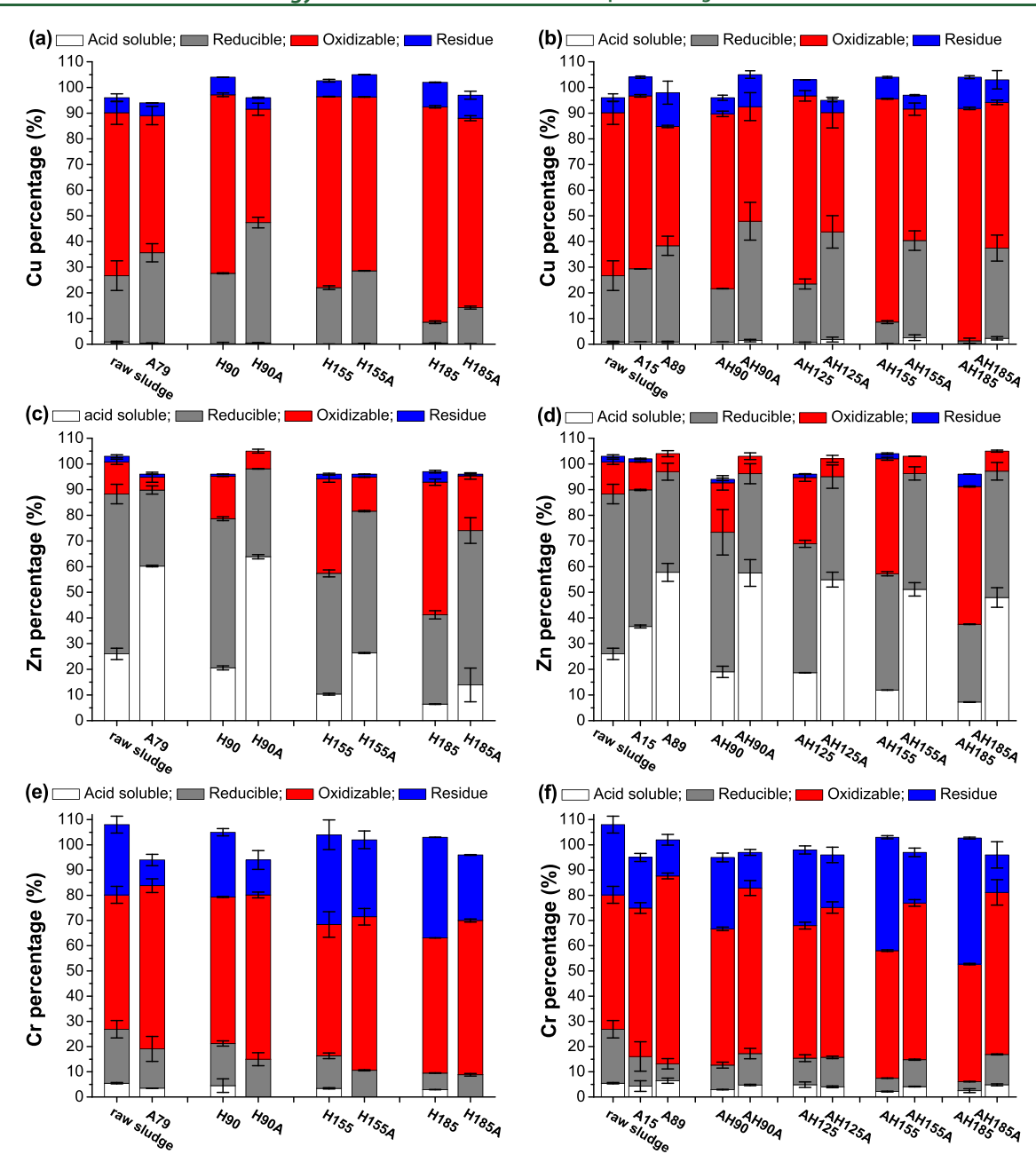


Figure 1. (a-f) Distribution of Cu, Zn, and Cr in the extracts/residue from sequential extraction of raw sludge, hydrochars, and AD solids. The relative abundance of each metal in the extracts/residue was calculated by its content in the extracts/residue divided by its total content in the solids before sequential chemical extraction (SCE). Error bars indicate the standard deviation of measurements (n = 4). Panels (a), (c), and (e) are for the HT-AD system; panels (b), (d), and (f) are for the AD-HT-AD system.

NaHCO $_3$ (1.4 g/L), anaerobic inoculum (2 g VS/L), and secondary wastewater effluent. The AD reactors were maintained at 35 °C for 79 days while being shaked at \sim 220 rpm. A control AD experiment was set up to digest raw sludge without HT.

At the end of AD, an aliquot of the final suspension was immediately transferred to an anaerobic chamber (COY) filled with 95% $N_2/5\%$ H_2 , where the solids (AD solids hereinafter) and supernatant (AD process water hereinafter) were separated using 0.45 μm membrane filters. The AD solids were air-dried in the anaerobic chamber and used for composition and structure analyses.

2.2.2. AD-HT-AD System. Raw sludge was first anaerobically digested for 15 days at 35 °C in a capped 9 L glass reactor

under magnetic stirring. The total suspension in the reactor was 6 L, containing raw sludge (10 g VS/L), NaHCO $_3$ (1.4 g/L), anaerobic inoculum (1 g VS/L), and secondary wastewater effluent.

The 15-day digested sludge suspension without centrifugation was further treated by sequential HT and a second-stage AD using the same procedures as in the HT-AD system. To investigate the effect of low-temperature thermal hydrolysis, an additional interstage HT was conducted at 125 $^{\circ}\text{C}$. The second-stage AD lasted 74 days. The 15-day digested sludge suspension without HT was anaerobically incubated with the same procedure and used as the control.

No medium was used in all AD incubations to avoid introducing metals into the sludge. Total biogas volume and

composition were monitored periodically throughout each AD stage; the results will be presented in a parallel study. AD lasted over 70 days till the production of biomethane reached a plateau. The detailed experimental procedures for the two systems were also described in our previous studies.^{28,29}

2.3. Sample Characterization. The dried raw sludge, hydrochars, and AD solids were characterized using SCE (Text S1 in the Supporting Information), bulk XAS, and micro-X-ray fluorescence microscopy (μ -XRF) coupled with μ -XAS (Text S2). A portion of each solid sample was ashed and digested by aqua regia for total metal concentration analysis. The changes in the total concentrations of Cu, Zn, and Cr are provided in Text S3. For bulk XAS, both Cu and Zn K-edge extended X-ray fine structure (EXAFS) and X-ray absorption near edge structure (XANES) analyses were conducted on dried sludge samples and corresponding reference compounds. Due to the low content of Cr (<100 ppm) in the samples, μ -XANES analysis was conducted for Cr analysis.

XAS data analysis used software Ifeffit.³⁰ Principal component analysis (PCA) in combination with target transformation (TT) was conducted on the processed spectra using a suite of reference compounds to determine the number and identity of end member components for the subsequent linear combination fitting (LCF). The goodness of fitting was determined by an *R*-factor, and the fits with the smallest *R*-factors are reported. Details on the Cu, Zn, and Cr reference compounds for LCF analyses are in Table S1 and Figure S1.

3. RESULTS

3.1. Cu, Zn, and Cr Fractions by SCE Analysis. *3.1.1. Cu Fraction.* As shown in Figure 1a and b, Cu predominantly exists in the reducible (25.8%) and oxidizable (63.5%) fractions in raw sludge. For the HT-AD system, Cu speciation in sample HT90 is similar to raw sludge. However, HT at high temperatures (155 and 185 °C) decreased the reducible fraction and increased the oxidizable fraction of Cu. This change is more significant at higher HT temperatures. The reducible and oxidizable fractions of Cu in sample H185 are 8.1 and 83.9%, respectively. After the subsequent AD (sample H185A), the reducible fraction of Cu increased slightly to 14.1%, whereas the oxidizable fraction decreased to 73.8%.

For the AD-HT-AD system, Cu speciation is similar to raw sludge after the first-stage AD. The trends in the subsequent HT and second-stage AD are similar to those in the HT-AD system. Compared with the HT-AD system, HT hydrochars in the AD-HT-AD system have less reducible fraction but more oxidizable fraction of Cu. The second-stage AD solids have more reducible fraction but less oxidizable fraction of Cu than those derived from the HT-AD system.

3.1.2. Zn Fraction. As shown in Figure 1c and d, Zn predominantly exists in reducible (62.2%), acid-soluble (26.0%), and oxidizable (12.6%) fractions in raw sludge. For the HT-AD system, HT increased the oxidizable fraction and decreased the soluble and reducible fractions of Zn as compared to raw sludge. For instance, the acid-soluble, reducible, and oxidizable fractions in sample H185 are 6.4, 34.8, and 51.7%, respectively. After AD, the acid-soluble fraction in samples A79 and H90A increases significantly, while the reducible and oxidizable fractions decrease. For instance, the acid-soluble, reducible, and oxidizable fractions of Zn in sample H90A are 63.9, 34.2, and 6.9%, respectively. However, for samples H155A and H185A, the acid-soluble and reducible fractions of Zn increase, while the oxidizable fraction decreases

as compared to their corresponding hydrochars. The acid-soluble, reducible, and oxidizable fractions of Zn in sample H185A are 13.9, 60.2, and 21.2%, respectively.

For the AD-HT-AD system, after the first-stage AD, the Zn fractions are similar to those in raw sludge. The acid-soluble, reducible, and oxidizable fractions of Zn in sample A15 are 36.7, 53.2, and 10.9%, respectively. Similar trends for HT hydrochars and final AD solids are observed as those in the HT-AD system. Compared to the HT-AD system at high HT temperatures (155 and 185 $^{\circ}$ C), more soluble but less reducible fractions of Zn in the final AD solids are observed in the AD-HT-AD system.

3.1.3. Cr Fraction. As shown in Figure 1e and f, Cr fractions in raw sludge are 5.5% acid-soluble, 21.4% reducible, 53.3% oxidizable, and 27.8% residual. For the HT-AD system, compared with raw sludge, HT decreased both acid-soluble and reducible fractions while increased the residual fraction of Cr. The change in the oxidizable fraction is subtle after HT. For instance, the acid-soluble, reducible, oxidizable, and residue fractions of Cr in sample H185 are 2.9, 6.6, 53.6, and 39.9%, respectively. After the subsequent AD, the changes in the acid-soluble and reducible fractions are insignificant. However, the residue fraction significantly decreased (e.g., from 39.9% in sample H185 to 26% in sample H185A), while the oxidizable fraction increased (e.g., from 53.6% in sample H185 to 61.2% in sample H185A).

For the AD-HT-AD system, after the first-stage AD, the Cr fractions are similar to those in raw sludge. The acid-soluble, reducible, oxidizable, and residue fractions of Cr in sample A15 are 4.3, 11.7, 58.9, and 20.0%, respectively. Similar trends for HT hydrochars and final AD solids are observed to the HT-AD system. Compared with the HT-AD system conducted at high HT temperatures (155 and 185 °C), the residue fraction of Cr in HT hydrochars and the fractions of acid-soluble and reducible Cr in the final AD solids are higher in the AD-HT-AD system.

3.2. Cu Speciation by XAS. Cu XANES is used to probe in situ speciation information. For the HT-AD system (Figure S4a), a shoulder at 8982 eV in the spectra of HT hydrochars became pronounced as compared to raw sludge, indicating the presence of Cu(I) in the samples. Meanwhile, the shoulder at 8992 eV became weaker (Figure S4) due to less Cu(II) in HT hydrochars. These changes are consistent with a previous study showing the absorption features of Cu(I, II) compounds.³ The presence of the shoulder at 8982 eV in the spectra of sample A79 was also observed as compared to raw sludge (Figure S4). Moreover, the main peak and pre-edge peak of sample A79 significantly shifted to lower energy as compared to raw sludge, suggesting the reduction of Cu(II) to Cu(I) during AD. The first derivative of Cu K-edge XANES spectra of solid samples is also provided in Figure S5. The peak maximum of the first derivative of sample A79 slightly shifted to lower energy as compared to raw sludge, confirming the reduction of Cu(II) during AD. Similar changes are observed for samples H90A, H155A, and H185A as compared to their corresponding HT hydrochars. Such energy shifting is less significant for the AD solids after high-temperature HT, suggesting that high-temperature HT inhibited the degree of Cu(II) reduction during the subsequent AD.

For the AD-HT-AD system (Figure S4b), in addition to the absence of a shoulder at 8982 eV, the main peak and pre-edge peak of sample A15 did not shift as compared to raw sludge, suggesting that the 15-day duration of the first-stage AD did

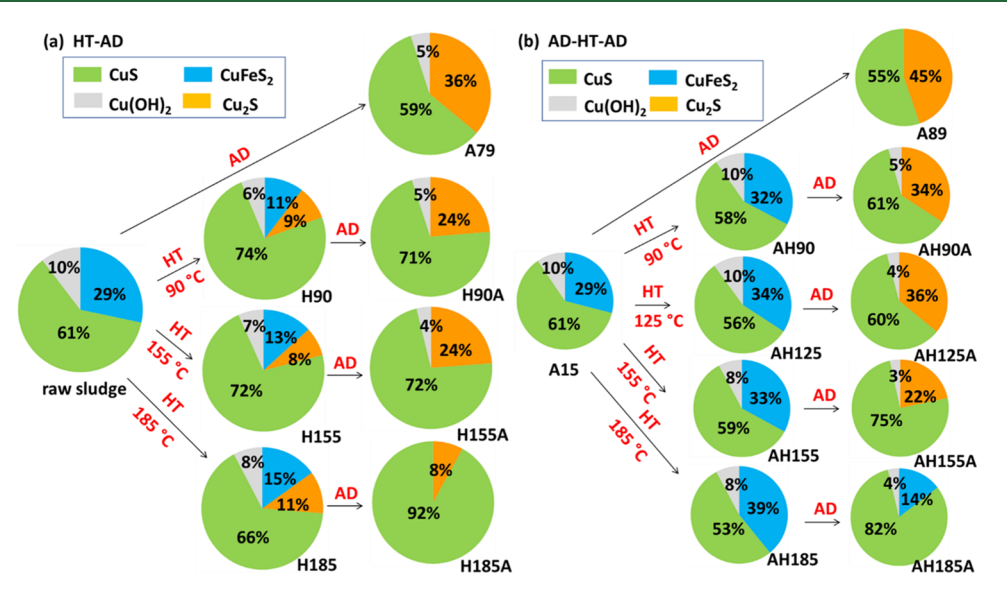


Figure 2. Relative abundance of Cu species determined from linear combination fitting (LCF) analysis of Cu K-edge XANES of the solid samples from (a) HT-AD and (b) AD-HT-AD systems. Fitting results are also reported in Table S2.

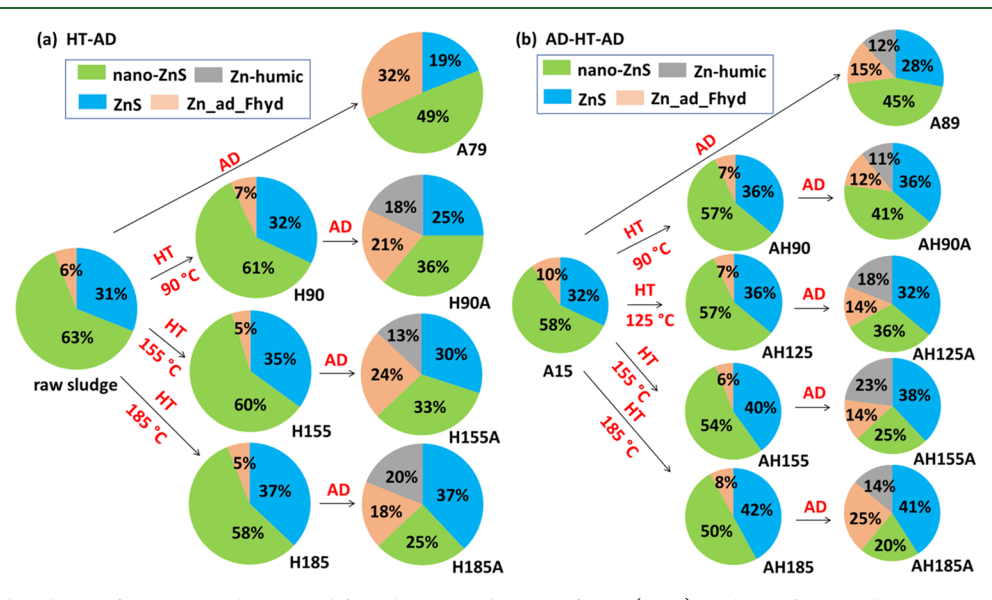


Figure 3. Relative abundance of Zn species determined from linear combination fitting (LCF) analysis of Zn K-edge XANES of the solid samples from (a) HT-AD and (b) AD-HT-AD systems. Fitting results are also reported in Table S4.

not induce Cu(II) reduction. The trends of energy shifting in Cu XANES spectra (and related redox state of Cu) for the subsequent HT hydrochars and final AD solids are similar to those in the HT-AD system.

We further conducted LCF analysis of Cu XANES using a large library of reference compounds to quantify Cu speciation in the solids. Based on previous studies on Cu speciation in sludge, 15,18,31,32 our reference compounds included Cu sulfides, $\text{Cu}(\text{OH})_2$, Cu-phosphate, Cu adsorbed on ferrihydrite (Cu_ad_Fhyd), a Cu-humic complex, etc. (Table S1 and Figure S1). Our fitting results revealed that the Cu-humic complex, Cu-phosphate, and Cu adsorbed on ferrihydrite were not significant components. The use of reference compounds Cu_2S , CuS, chalcopyrite, and $\text{Cu}(\text{OH})_2$ yielded the best fitting results. Note that the oxidation state of Cu in chalcopyrite is best considered to be $\text{Cu}^{\text{II}}\text{Fe}^{\text{II}}\text{S}_2$ based on XAS analysis. 33,34 Cu is present predominantly as sulfides (CuS 54.3% and

chalcopyrite 34.5%) and $Cu(OH)_2$ (11.2%) in raw sludge (Figure 2a and Table S2).

For the HT-AD system (Figure 2a, Figure S6a, and Table S2), Cu sulfides are the predominant species in the hydrochars similar to raw sludge. However, CuS slightly increases and chalcopyrite decreases in fractions in the HT hydrochars. For instance, the fractions of CuS, chalcopyrite, and $\text{Cu}(\text{OH})_2$ in sample H185 are 79.8, 11.0, and 9.2%, respectively. Cu sulfides still dominate in the subsequent AD solids, but only Cu_2S is present. The fraction of Cu_2S decreases in the AD solids following high-temperature HT. For instance, the fractions of CuS (66%) and Cu_2S (27.3%) in sample A79 decrease to CuS (93.7%) and Cu_2S (6.3%) in sample H185A.

For the AD-HT-AD system (Figure 2b, Figure S6b, and Table S2), after the first-stage AD, Cu sulfide is the predominant species in sample A15, similar to raw sludge. However, 11.4% of ferrihydrite-adsorbed Cu is also present.

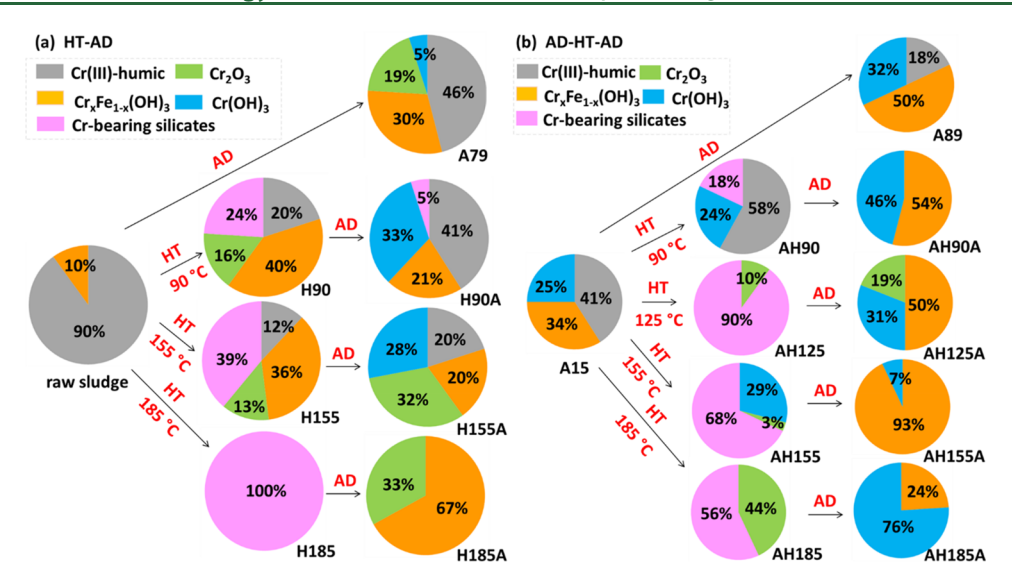


Figure 4. Relative abundance of Cr species determined from linear combination fitting (LCF) analysis of Cr K-edge μ -XANES data of the solid samples from (a) HT-AD and (b) AD-HT-AD systems. The value for each sample is averaged over two or three hot spots reported in Table S6.

The transformation of Cu for the subsequent HT hydrochars and AD solids is similar to those in the HT-AD system.

Cu EXAFS spectra are generally noisy due to the low concentration of Cu in the solid samples (Figure S7), but we still observed the transformation of chalcopyrite into CuS and Cu₂S, as well as the inhibitory effect of high-temperature HT on Cu₂S formation during the subsequent AD (Table S3). Note that some Cu species with fractions below 10% are kept for XAS LCF analyses, in order to comparatively evaluate the trends of the Cu speciation change in the sludge during HT/AD using the same combination of reference compounds. Considering that the error of XAS LCF analyses is typically $\sim\!10\%$, Cu species with a low fraction might exist in the solid samples. These same considerations were also applied to Zn and Cr XAS LCF analyses below.

3.3. Zn Speciation by XAS. For the HT-AD system (Figure S8a), the Zn XANES spectra of hydrochars are comparable to that of raw sludge. However, the main peak of the subsequent AD solids was flattened as compared to their corresponding hydrochars. For the AD-HT-AD system (Figure S8b), the spectra of the A15 sample are similar to that of raw sludge, suggesting that the first-stage AD did not change Zn speciation. The changes of Zn XANES spectra for the subsequent hydrochars and final AD solids are similar to the HT-AD system. A large library of reference compounds based on previous studies 15,18,32,35 was employed for LCF analysis, including Zn sulfides, hopeite (Zn₃(PO₄)₂·4H₂O), Zn adsorbed on ferrihydrite (Zn ad Fhyd), a Zn-humic complex, etc. (Table S1 and Figure S1). The use of reference compounds nano-ZnS, sphalerite, Zn ad Fhyd, and a Znhumic complex yielded the best fitting results. Note that nano-ZnS was used for fitting as previous studies suggested it to be the main Zn sulfide phase in the sludge. 18,35 Sphalerite was chosen as a reference compound, as our previous studies showed that Fe content in raw sludge (same sludge used for this study) was much higher than other metals (i.e., Cu, Zn, and Cr) and Fe sulfides were the main inorganic S species in the hydrochars and AD solids. 28,29 Fe is also a common impurity in Zn sulfide phases. The choice of chalcopyrite as a reference compound for Cu XAS LCF analyses was for similar reasons. LCF analysis of Zn XANES shows that in raw sludge,

Zn predominantly exists as nano-ZnS (63%), sphalerite (31%), and a minor amount of Zn ad Fhyd (6%) (Figure 3a, Figure S9a, and Table S4). For the HT-AD system (Figure 3a, Figure S9a, and Table S4), HT did not change Zn speciation even at 185 °C. After the subsequent AD, Zn sulfides remain as the dominant Zn species in the AD solids. However, the total fractions of ferrihydrite-adsorbed Zn and the Zn-humic complex increase from ~6% in the hydrochars to 38% in the AD solids, whereas nano-ZnS decreases from ~60% in the hydrochars to ~30% in the AD solids. Compared with raw sludge, AD alone partially converted Zn sulfides to Zn ad Fhyd. The fractions of nano-ZnS, sphalerite, and Znadsorbed ferrihydrite in sample A79 are 48.8, 19.5, and 31.7%, respectively. Compared with sample A79, samples H90A, H155A, and H185A contain lower fractions of nano-ZnS but higher fractions of sphalerite, suggesting that prestage HT at 90-185 °C induced the dissolution of nano-ZnS during the subsequent AD.

For the AD-HT-AD system (Figure 3b, Figure S9b, and Table S4), the first-stage AD did not significantly change Zn speciation in sample A15 as compared to raw sludge. The changes in Zn speciation in the subsequent hydrochars and the final AD solids in the AD-HT-AD system are similar to the HT-AD system. LCF analysis of Zn EXAFS (Figure S10 and Table S5) shows slightly different values as compared to those derived from LCF analysis of XANES data (Table S4) but overall similar trends on the relative abundance of nano-ZnS and sphalerite. The differences in fitted nano-ZnS and sphalerite fractions are possibly due to the EXAFS spectral similarities of nano-ZnS and sphalerite (Figure S1).

3.4. Cr Speciation by XAS. The μ -XRF images of selected Cr hot spots are provided in Figure S11, showing that micrometer-sized Cr-containing particles/aggregates in the solids are distributed heterogeneously and preferentially associated with Fe and/or Si in hydrochars and AD solids. The corresponding Cr μ -XANES spectra are shown in Figure S12. For the HT-AD system, Cr XANES spectra of HT hydrochars and AD solids differ significantly from raw sludge. For the AD-HT-AD system, the spectra of sample A15, HT hydrochars, and AD solids are all different from sample A15.

To better represent Cr speciation in the bulk sample, we averaged the LCF results of μ -XANES from multiple hot spots (Figure 4). A large library of reference compounds based on previous studies^{36–38} was employed for the LCF analysis, including a Cr(III)-humic complex, Cr(III) (oxy)hydroxides, mixed Cr(III)-Fe(III) (oxy)hydroxides, Cr(III)-bearing silicate minerals, CaCrO₄, K₂CrO₄, etc. (Table S1 and Figure S1). The Cr(III)-humic complex (~90%) is the predominant species in raw sludge, with the rest being $Fe_xCr_{1-x}(OH)_3$ (sum of Fe_{0.9}Cr_{0.1}(OH)₃ and Fe_{0.2}Cr_{0.8}(OH)₃) (Figure 4a). No CaCrO₄ or K₂CrO₄ was fitted in raw sludge, consistent with previous studies showing that Cr(III) phases are the main Cr species in sewage sludge samples. ^{21,22} Cr(VI) compounds can also be readily reduced to Cr(III) by organics and bacteria in the activated sludge process. 39,40 For the HT-AD system (Figure 4a), no Cr(III)-humic complex was fitted in the 155 °C HT hydrochars, whereas the fractions of Cr2O3, $Fe_rCr_{1-r}(OH)_3$, and Cr(III)-bearing silicates (fuchsite and uvarovite) are high. The fraction of Cr₂O₃ also increases significantly with increasing HT temperature. For example, the dominant Cr species in sample H185 are Cr-bearing silicates (27%) and Cr_2O_3 (73%). The fraction of Cr-bearing silicates is very low in the AD solids, and the predominant Cr species are the Cr(III)-humic complex, Cr₂O₃, Cr(OH)₃, and $Fe_rCr_{1-r}(OH)_3$. For the AD alone sample, a portion of the Cr(III)-humic complex in raw sludge is converted to Cr₂O₃, $Cr(OH)_3$, and $Fe_xCr_{1-x}(OH)_3$ for sample A79.

Similarly, for the AD-HT-AD system, the first-stage AD converted a portion of the Cr(III)-humic complex in raw sludge into $Fe_xCr_{1-x}(OH)_3$ and $Cr(OH)_3$ for sample A15 (Figure 4b). The fraction of the Cr(III)-humic complex decreases and completely disappears in high-temperature HT hydrochars, whereas Cr-bearing silicates, Cr_2O_3 , and $Cr(OH)_3$ become the predominant species. For the second-stage AD, Cr-bearing silicates and Cr_2O_3 in HT hydrochars transform to $Fe_xCr_{1-x}(OH)_3$ and $Cr(OH)_3$ in the final AD solids. No Cr(VI) compounds were used for fitting the hydrochar and AD solid samples, as no Cr(VI) was observed in raw sludge and both HT and AD created reducing chemical and/or biological environments.

4. DISCUSSION

4.1. Transformation of Cu, Zn, and Cr during HT. In this study, both Zn and Cu exist predominantly as sulfides in raw sludge, similar to previous findings on their speciation in mixed primary sludge and waste-activated sludge. ^{15,32,35} Because HT also favors the sulfidation of Zn and Cu, ^{15,41} it is not surprising to find both elements remaining as sulfides in HT hydrochars similar to raw sludge.

For Zn speciation, nano-ZnS partially transforms to sphalerite during HT in both HT-AD and AD-HT-AD systems (Figure 3 and Table S4), likely due to the aging and recrystallization of nano-ZnS into the bulk crystalline phase.

For Cu speciation, in the HT-AD system, HT partially converts chalcopyrite (CuFeS $_2$) into CuS and Cu $_2$ S (Figure 2a). It is likely due to chalcopyrite dissolution in acidic ferric solution (eq 1) and subsequent precipitation of CuS (eq 2), where soluble Fe $^{3+}$ and S $^{2-}$ can be produced from the dissolution of an Fe(III)-OM complex and hydrolysis of organic S during HT, respectively. 28

$$CuFeS_2 + 4Fe^{3+} \leftrightarrow Cu^{2+} + 5Fe^{2+} + 3S$$
 (1)

$$Cu^{2+} + S^{2-} \rightarrow CuS \tag{2}$$

$$Fe^{2+} + S^{2-} \rightarrow FeS \tag{3}$$

In addition, the produced Cu^{2+} can also be reduced by hydroxymethylfurfural (5-HMF)⁴³ or hydroquinones of fulvic acid, 44,45 producing Cu^+ that can precipitate as Cu_2S . In the AD-HT-AD system, little conversion of chalcopyrite into CuS/Cu_2S was observed at 90–155 °C HT due to the alkaline environment during reaction (Table 1) as well as the presence of little amount of Fe^{3+} (the first-stage AD induced Fe(III) reduction to Fe(II)) available for chalcopyrite dissolution through eq 1.²⁹ We also observe partial replacement of CuS by chalcopyrite at HT 185 °C, possibly due to the reaction between FeS and CuS.

For Cr speciation, the Cr(III)-organic complex is the predominant Cr species in raw sludges. 22 Cr₂O₃ is previously observed to occur during HT at 100–180 °C through the decomposition of the Cr(III)-organic complex. 46 Sewage sludge, rich in Si and Al, 4,47 can also enable the formation of low-solubility Cr-bearing silicate phases during HT, such as the fuchsite and uvarovite observed in this study (Table S6). A recent study showed that Cr(III)-bearing silicates can accumulate during Cr phase transformation in hydrothermal slurries. 48 We also observed the precipitation of Fe_xCr_{1-x}(OH)₃, which is a common environmental sink phase of Cr(III) and has lower solubility than pure Cr(OH)₃. 36,37

Interestingly, despite the different species observed by XAS for Cu, Zn, and Cr, SCE reveals that the relative abundance of Cu, Zn, and Cr in aqueous extracts and solid residues from sequential extraction of solid samples in HT-AD and AD-HT-AD systems is comparable. HT of raw sludge at pH 6.34 (HT-AD system) and A15 at pH 7.60 (AD-HT-AD system) decreases acid-soluble and reducible fractions of Cu, Zn, and Cr in HT hydrochars but increases the oxidizable and residue fractions, in agreement with previous studies on the transformation of Cu, Zn, and Cr during HT of sewage sludge. The high acid-soluble fraction of Zn in HT hydrochars is likely due to the presence of nano-ZnS, which has high surface area and many defect sites that are highly reactive and susceptible to dissolution such as under acidic conditions.

4.2. Transformation of Cu, Zn, and Cr during AD. Cu is commonly present as Cu sulfides in sludge, including CuFeS₂, CuS, and Cu₂S. Their solubility follows the order of CuFeS₂ > Cu₂S > CuS. ⁵¹ Cu preferentially exists in its most reducible form (i.e., Cu₂S) in anaerobically digested sludge. ^{52,53} A recent study reported the reduction of Cu(II) and formation of Cu₂S during AD. ¹⁸ Anaerobic sulfate-reducing bacteria (SRB) can be involved in the transformation of chalcopyrite into ferrous sulfides and soluble Cu(II) under anaerobic conditions. ⁵⁴ The released Cu(II) can then be reduced by 5-HMF derived from HT of sludge or hydroquinone-like moieties in organic matter of sewage sludge. ⁵⁵ A recent study also showed that AD promotes the transformation of chalcopyrite into Cu₂S. ³¹

During AD alone (control), CuFeS₂ is transformed to CuS and Cu₂S in samples A79 and A89, whereas it is absent in sample A15 (Figure 2). This suggests that 15-day AD is not long enough to induce the transformation of CuFeS₂, suggesting that transformation of CuFeS₂ during AD is a slow process. AD of HT hydrochar slurries from higher HT temperatures (155 and 185 °C) results in the formation of less Cu₂S but more CuS, likely due to the lower concentrations of

organic matter as electron donors in these samples. Our recent study showed that increasing HT temperature produces hydrochars with more polyaromatic hydrocarbon networks, which are not easily oxidized during AD. This is also consistent with our recent observations that HT at higher temperatures induced less vivianite $(Fe_3(PO_4)_2)$ formation during the subsequent AD, where the concentration of Fe in sewage sludge is 45.5 times higher than that of Cu. ²⁸

ZnS/nano-ZnS is previously shown to be the predominant Zn species in AD solids. 18,56,57 Our results show the partial transformation of nano-ZnS into adsorbed species (e.g., Zn adsorbed on ferrihydrite) and an organic complex (e.g., Znhumic complex) during AD. Compared with ZnS, nano-ZnS has higher total surface free energy, making the surface Zn atoms highly reactive and prone to dissolution.^{35,58} Previous studies showed the transformation of ZnS into ligand complexes such as $Zn(OH)_m(HS)_n$ or Zn-thiolate in alkaline sulfidic solutions under anaerobic conditions. 59,60 This is consistent with the high fraction of the Zn-humic complex identified from LCF of Zn XANES in this study, as well as the high sulfide concentration in AD process water reported in our parallel studies. 28,29 For AD alone, the transformation of nano-ZnS in the 15-day AD is slower than that in the 79 and 89-day AD, probably due to the shorter reaction time.

Fuchsite and uvarovite formed in HT hydrochars are Cr(III)-bearing silicate minerals. Multiple microbial species can lead to the dissolution of silicate minerals. Moreover, alkaline conditions favor the dissolution of Cr(III)-bearing silicate minerals, ^{63,64} and the pH values are higher than 7 during AD (Table 1). The produced Cr^{3+} then precipitates as $Cr(OH)_3$ or the $Fe_xCr_{1-x}(OH)_3$ solid solution under alkaline conditions. ^{65,66}

For SCE analyses, Cu and Cr predominantly exist as the reducible and oxidizable fractions in the AD solids, whereas Zn predominantly exists as acid-extractable and reducible fractions. These observations are consistent with previous studies on Cu, Zn, and Cr speciation in anaerobically digested sludge. The high fraction of acid-soluble Zn in AD solids is due to the dissolution of nano-ZnS, desorption of Zn from ferrihydrite, and break down of the Zn-humic complex during acetic acid extraction.

Overall, the first-stage AD (15 days) in the AD-HT-AD system does not significantly change the predominant species of Cu and Zn. Thus, the transformation trends of Cu and Zn in the HT-AD and AD-HT-AD systems are similar. For Cr, the first stage transformed a portion of the Cr(III)-humic complex into $Fe_xCr_{1-x}(OH)_3$ and $Cr(OH)_3$, but the dominant reaction pathways during the AD-HT-AD system are similar to the HT-AD system. However, some differences (i.e., types and contents of some metal species) in the AD-HT-AD system are observed as compared to the HT-AD system because the first-stage AD changed the sludge matrix. For instance, the speciation of Fe, S, and C and pH in the 15-day digested sludge are different from those in raw sludge, 28,29 and such differences can affect the evolution pathways of other elements during the subsequent treatments. For example, our results shed light on the role of Fe in the transformation of Cu, Zn, and Cr during the combined HT/AD.

4.3. Comparison of XAS and SCE. This study employed both XAS and SCE to provide complement speciation and mobility information on the metals of interest. Synchrotron XAS analysis (including LCF analysis) is a well-established method for determining elemental speciation such as the

oxidation state, coordination environment, and phase, but this method has intrinsic limitations with a general error range of ~10%. The uncertainty of LCF analysis is potentially caused by (1) the similarities in XAS spectra of some reference compounds and (2) the difficulties in building a complete library of reference compounds for highly complex and heterogeneous samples such as sludge. Moreover, XAS LCF analysis alone does not provide direct mobility information as SCE. On the other hand, SCE also has some limitations, 15,68 for instance (1) SCE cannot directly identify and quantify metal species in mineral phases due to nonspecific dissolution and potential speciation alteration during extraction. For instance, as discussed above, SCE showed that the high acidsoluble fraction of Zn in HT hydrochars and AD solids was due to the dissolution of nano-ZnS, desorption of Zn from ferrihydrite, and decomposition of the Zn-humic complex during acetic acid extraction. (2) The chemical oxidation state cannot be accurately reflected. For instance, SCE failed to observe the reduction of Cu(II) during the AD process. (3) The extraction efficiency is strongly affected by the sample matrix such as the aggregation state of the solid samples, pH, and particle size. 69 (4) It is difficult to quantify metals associated with specific minerals due to the nonselectivity of extraction reagents and redistribution of analytes and the possible newly formed precipitates during the extraction.

With the intrinsic limitations of the two methods, it is thus important to combine them in order to obtain a better understanding of such complex matrices. XAS as an *in situ*, nondestructive, and highly sensitive method can provide information on the molecular-scale chemical state of an element, which can be used to trace the chemical environment during such complex and sequential treatment processes, whereas SCE as an empirical method provides more insights into the potential mobility and bioavailability of the solid phases upon contact with environmental media.

4.4. Environmental Implications. This study showed that HT affects the mobility of Cu, Zn, and Cr and promotes the formation of low-solubility Cu and Zn sulfides, Cr₂O₃, and Cr-bearing silicates. High HT temperatures (155 and 185 °C) favor the formation of lower mobility and bioavailability phases of Cu, Zn, and Cr.

Long-term AD (i.e., 74 or 79 days) favors the reductive transformation of CuFeS₂ into Cu₂S and the partial conversion of nano-ZnS into ferrihydrite-adsorbed Zn and the Zn-organic complex. Pre- and interstage HT at high temperatures (155 and 185 °C) inhibit the formation of Cu₂S but enhance the conversion of nano-ZnS during the subsequent AD. It is important to note that a substantial amount of nano-ZnS is present in HT hydrochars and AD solids. Nano-ZnS is previously shown to be unstable and may pose environmental risks through dissolution at low pH,⁴⁹ with strong ligands,⁵⁸ or under aerobic conditions.³⁵ Ferrihydrite-sorbed Zn and the Zn-humic complex can release Zn into the environment through desorption or organic matter mineralization, respectively.^{18,35}

The predominant Cr species in AD solids are the Cr(III)-humic complex, Fe $_x$ Cr $_{1-x}$ (OH) $_3$, and Cr(OH) $_3$. Although Fe $_x$ Cr $_{1-x}$ (OH) $_3$ and Cr(OH) $_3$ are the low-solubility phases of Cr, previous studies have shown that organic ligands (i.e., siderophores and oxalate) can promote the dissolution of Fe $_x$ Cr $_{1-x}$ (OH) $_3$ and Cr(OH) $_3$. The released soluble Cr(III) and the Cr(III)-OM complex are susceptible to oxidation by environmental Mn oxides to form toxic Cr(VI) species.

This study provides an improved understanding on the chemical and biological processes involved in sludge management techniques using combined AD/HT. The results provide insights for the selection and optimization of treatment conditions that can balance the needs for energy and nutrient recovery as well as contaminant immobilization. Considering the importance of heavy metals for final sludge application or disposal,4 the transformation and mobility of heavy metals throughout their life cycle (i.e., in raw sludge, during treatment, and upon disposal or land application in the soil environment) warrant future investigation, such as the stability of metal sulfides during sludge land application under various soil conditions (e.g., varied pH, the presence of organics, and redox fluctuations). For instance, low-solubility Cu sulfides are the predominant Cu species in AD solids, but the fate of metal sulfides in soil conditions upon land application of AD solids remains unclear.18

ASSOCIATED CONTENT

Solution Supporting Information

The Supporting Information is available free of charge at https://pubs.acs.org/doi/10.1021/acs.est.0c05164.

Texts for SCE analysis, XAS analyses, and changes in the total concentrations of Cu, Zn, and Cr; table and figure for reference compounds used for XAS LCF analyses; tables and figures for Cu, Zn, and Cr XAS analyses of raw sludge, HT hydrochars, and AD solids (PDF)

AUTHOR INFORMATION

Corresponding Author

Yuanzhi Tang — School of Earth and Atmospheric Sciences, Georgia Institute of Technology, Atlanta, Georgia 30332-0340, United States; School of Civil and Environmental Engineering, Georgia Institute of Technology, Atlanta, Georgia 30332-0512, United States; oocid.org/0000-0002-7741-8646; Phone: 404-894-3814; Email: yuanzhi.tang@eas.gatech.edu

Authors

Qian Wang — School of Earth and Atmospheric Sciences, Georgia Institute of Technology, Atlanta, Georgia 30332-0340, United States

Chiqian Zhang — School of Civil and Environmental Engineering, Georgia Institute of Technology, Atlanta, Georgia 30332-0512, United States; orcid.org/0000-0003-4532-7376

Haesung Jung — School of Earth and Atmospheric Sciences, Georgia Institute of Technology, Atlanta, Georgia 30332-0340, United States; orcid.org/0000-0002-8795-248X

Pan Liu – School of Earth and Atmospheric Sciences, Georgia Institute of Technology, Atlanta, Georgia 30332-0340, United States

Dhara Patel – School of Earth and Atmospheric Sciences, Georgia Institute of Technology, Atlanta, Georgia 30332-0340, United States

Spyros G. Pavlostathis — School of Civil and Environmental Engineering, Georgia Institute of Technology, Atlanta, Georgia 30332-0512, United States; orcid.org/0000-0001-9731-3836

Complete contact information is available at: https://pubs.acs.org/10.1021/acs.est.0c05164

Notes

The authors declare no competing financial interest.

ACKNOWLEDGMENTS

This work was supported by the U.S. National Science Foundation under grant no. 1739884 (Y.T.). We acknowledge beamline scientists at beamlines 4-1 and 2-3 at the Stanford Synchrotron Radiation Lightsource (SSRL), 12-BM at the Advanced Photon Source (APS), and 5-ID at the National Synchrotron Light Source II (NSLS-II) for assistance in data collection. This research used resources of the SSRL, APS, and NSLS-II, U.S. Department of Energy (DOE) Office of Science User Facilities operated under contract nos. DE-AC02-76SF00515, DE-AC02-06CH11357, and DE-SC0012704, respectively.

REFERENCES

- (1) Peccia, J.; Westerhoff, P. We should expect more out of our sewage sludge. *Environ. Sci. Technol.* **2015**, 49, 8271–8276.
- (2) Paez-Rubio, T.; Peccia, J. Quantification of airborne biological contaminants associated with land-applied biosolids; Water Environment Research Foundation, Tempe, AZ: 2007.
- (3) Rogers, H. R. Sources, behaviour and fate of organic contaminants during sewage treatment and in sewage sludges. *Sci. Total Environ.* **1996**, *185*, 3–26.
- (4) Westerhoff, P.; Lee, S.; Yang, Y.; Gordon, G. W.; Hristovski, K.; Halden, R. U.; Herckes, P. Characterization, recovery opportunities, and valuation of metals in municipal sludges from U.S. wastewater treatment plants nationwide. *Environ. Sci. Technol.* **2015**, *49*, 9479–9488.
- (5) Wilfert, P.; Kumar, P. S.; Korving, L.; Witkamp, G.-J.; van Loosdrecht, M. C. M. The relevance of phosphorus and iron chemistry to the recovery of phosphorus from wastewater: A review. *Environ. Sci. Technol.* **2015**, *49*, 9400–9414.
- (6) Pavlostathis, S. G. Kinetics and modeling of anaerobic treatment and biotransformation processes. *Compr. Biotechnol.* **2011**, *6*, 385–307
- (7) Pavlostathis, S. G.; Giraldo-Gomez, E. Kinetics of anaerobic treatment: A critical review. *Crit. Rev. Environ. Control* **1991**, 21, 411–490.
- (8) Berge, N. D.; Ro, K. S.; Mao, J.; Flora, J. R. V.; Chappell, M. A.; Bae, S. Hydrothermal carbonization of municipal waste streams. *Environ. Sci. Technol.* **2011**. 45, 5696–5703.
- (9) Akiya, N.; Savage, P. E. Roles of water for chemical reactions in high-temperature water. *Chem. Rev.* **2002**, *102*, 2725–2750.
- (10) Appels, L.; Degrève, J.; Van der Bruggen, B.; Van Impe, J.; Dewil, R. Influence of low temperature thermal pre-treatment on sludge solubilisation, heavy metal release and anaerobic digestion. *Bioresour. Technol.* **2010**, *101*, 5743–5748.
- (11) Ortega-Martinez, E.; Sapkaite, I.; Fdz-Polanco, F.; Donoso-Bravo, A. From pre-treatment toward inter-treatment. Getting some clues from sewage sludge biomethanation. *Bioresour. Technol.* **2016**, 212, 227–235.
- (12) Barber, W. P. F. Thermal hydrolysis for sewage treatment: A critical review. *Water Res.* **2016**, *104*, 53–71.
- (13) Hii, K.; Baroutian, S.; Parthasarathy, R.; Gapes, D. J.; Eshtiaghi, N. A review of wet air oxidation and thermal hydrolysis technologies in sludge treatment. *Bioresour. Technol.* **2014**, *155*, 289–299.
- (14) Mossop, K. F.; Davidson, C. M. Comparison of original and modified BCR sequential extraction procedures for the fractionation of copper, iron, lead, manganese and zinc in soils and sediments. *Anal. Chim. Acta* **2003**, *478*, 111–118.
- (15) Huang, R.; Zhang, B.; Saad, E. M.; Ingall, E. D.; Tang, Y. Speciation evolution of zinc and copper during pyrolysis and hydrothermal carbonization treatments of sewage sludges. *Water Res.* **2018**, *132*, 260–269.

- (16) Wong, S. C.; Li, X. D.; Zhang, G.; Qi, S. H.; Min, Y. S. Heavy metals in agricultural soils of the Pearl River Delta, South China. *Environ. Pollut.* **2002**, *119*, 33–44.
- (17) Cheng, Y.; Luo, L.; Lv, J.; Li, G.; Wen, B.; Ma, Y.; Huang, R. Copper speciation evolution in swine manure induced by pyrolysis. *Environ. Sci. Technol.* **2020**, *54*, 9008–9014.
- (18) Legros, S.; Levard, C.; Marcato-Romain, C.-E.; Guiresse, M.; Doelsch, E. Anaerobic digestion alters copper and zinc speciation. *Environ. Sci. Technol.* **2017**, *51*, 10326–10334.
- (19) Dong, B.; Liu, X.; Dai, L.; Dai, X. Changes of heavy metal speciation during high-solid anaerobic digestion of sewage sludge. *Bioresour. Technol.* **2013**, *131*, 152–158.
- (20) Liu, T.; Liu, Z.; Zheng, Q.; Lang, Q.; Xia, Y.; Peng, N.; Gai, C. Effect of hydrothermal carbonization on migration and environmental risk of heavy metals in sewage sludge during pyrolysis. *Bioresour. Technol.* **2018**, 247, 282–290.
- (21) Fadiran, A. O.; Tiruneh, A. T.; Mtshali, J. S. Assessment of mobility and bioavailability of heavy metals in sewage sludge from Swaziland through speciation analysis. *Am. J. Environ. Prot.* **2014**, *3*, 198–208.
- (22) Jin, R.; Liu, Y.; Liu, G.; Tian, T.; Qiao, S.; Zhou, J. Characterization of product and potential mechanism of Cr(VI) reduction by anaerobic activated sludge in a sequencing batch reactor. *Sci. Rep.* **2017**, *7*, 1681–1681.
- (23) Liu, M.; Duan, Y.; Bikane, K.; Zhao, L. The migration and transformation of heavy metals in sewage sludge during hydrothermal carbonization combined with combustion. *BioMed Res. Int.* **2018**, 2018, 1913848.
- (24) Shi, W.; Liu, C.; Shu, Y.; Feng, C.; Lei, Z.; Zhang, Z. Synergistic effect of rice husk addition on hydrothermal treatment of sewage sludge: Fate and environmental risk of heavy metals. *Bioresour. Technol.* **2013**, *149*, 496–502.
- (25) Kasiuliene, A.; Carabante, I.; Bhattacharya, P.; Kumpiene, J. Hydrothermal carbonisation of peat-based spent sorbents loaded with metal(loid)s. *Environ. Sci. Pollut. Res.* **2019**, *26*, 23730–23738.
- (26) Zhai, Y.; Liu, X.; Zhu, Y.; Peng, C.; Wang, T.; Zhu, L.; Li, C.; Zeng, G. Hydrothermal carbonization of sewage sludge: The effect of feed-water pH on fate and risk of heavy metals in hydrochars. *Bioresour. Technol.* **2016**, *218*, 183–188.
- (27) Fang, C.; Huang, R.; Dykstra, C. M.; Jiang, R.; Pavlostathis, S. G.; Tang, Y. Energy and nutrient recovery from sewage sludge and manure via anaerobic digestion with hydrothermal pretreatment. *Environ. Sci. Technol.* **2020**, *54*, 1147–1156.
- (28) Wang, Q.; Zhang, C.; Patel, D.; Jung, H.; Liu, P.; Wan, B.; Pavlostathis, S. G.; Tang, Y. Coevolution of iron, phosphorus, and sulfur speciation during anaerobic digestion with hydrothermal pretreatment of sewage sludge. *Environ. Sci. Technol.* **2020**, *54*, 8362–8372.
- (29) Wang, Q.; Zhang, C.; Liu, P.; Jung, H.; Wan, B.; Patel, D.; Pavlostathis, S. G.; Tang, Y. Effect of inter-stage hydrothermal treatment on anaerobic digestion of sewage sludge: Speciation evolution of phosphorus, iron, and sulfur. ACS Sustainable Chem. Eng. 2020, 8, 16515–16525.
- (30) Ravel, B.; Newville, M. ATHENA, ARTEMIS, HEPHAESTUS: data analysis for X-ray absorption spectroscopy using IFEFFIT. *J. Synchrotron Radiat.* **2005**, *12*, 537–541.
- (31) Legros, S.; Chaurand, P.; Rose, J.; Masion, A.; Briois, V.; Ferrasse, J.-H.; Macary, H. S.; Bottero, J.-Y.; Doelsch, E. Investigation of copper speciation in pig slurry by a multitechnique approach. *Environ. Sci. Technol.* **2010**, *44*, 6926–6932.
- (32) Donner, E.; Howard, D. L.; Jonge, M. D. d.; Paterson, D.; Cheah, M. H.; Naidu, R.; Lombi, E. X-ray absorption and micro X-ray fluorescence spectroscopy investigation of copper and zinc speciation in biosolids. *Environ. Sci. Technol.* **2011**, *45*, 7249–7257.
- (33) Todd, E. C.; Sherman, D. M.; Purton, J. A. Surface oxidation of chalcopyrite (CuFeS₂) under ambient atmospheric and aqueous (pH 2-10) conditions: Cu, Fe L- and O K-edge X-ray spectroscopy. *Geochim. Cosmochim. Acta* **2003**, *67*, 2137–2146.

- (34) Mikhlin, Y.; Tomashevich, Y.; Tauson, V.; Vyalikh, D.; Molodtsov, S.; Szargan, R. A comparative X-ray absorption nearedge structure study of bornite, Cu₅FeS₄, and chalcopyrite, CuFeS₂. *J. Electron Spectrosc. Relat. Phenom.* **2005**, *142*, 83–88.
- (35) Le Bars, M.; Legros, S.; Levard, C.; Chaurand, P.; Tella, M.; Rovezzi, M.; Browne, P.; Rose, J.; Doelsch, E. Drastic change in zinc speciation during anaerobic digestion and composting: instability of nano-sized zinc sulfide. *Environ. Sci. Technol.* **2018**, *52*, 12987–12996.
- (36) Saad, E. M.; Sun, J.; Chen, S.; Borkiewicz, O. J.; Zhu, M.; Duckworth, O. W.; Tang, Y. Siderophore and organic acid promoted dissolution and transformation of Cr(III)-Fe(III)-(oxy)hydroxides. *Environ. Sci. Technol.* **2017**, *51*, 3223–3232.
- (37) Tang, Y.; Michel, F. M.; Zhang, L.; Harrington, R.; Parise, J. B.; Reeder, R. J. Structural properties of the Cr(III)–Fe(III) (Oxy)-hydroxide compositional series: insights for a nanomaterial "solid solution". *Chem. Mater.* **2010**, *22*, 3589–3598.
- (38) Aldmour, S. T.; Burke, I. T.; Bray, A. W.; Baker, D. L.; Ross, A. B.; Gill, F. L.; Cibin, G.; Ries, M. E.; Stewart, D. I. Abiotic reduction of Cr(VI) by humic acids derived from peat and lignite: kinetics and removal mechanism. *Environ. Sci. Pollut. Res.* **2019**, *26*, 4717–4729.
- (39) Hsu, L. C.; Wang, S. L.; Lin, Y. C.; Wang, M. K.; Chiang, P. N.; Liu, J. C.; Kuan, W. H.; Chen, C. C.; Tzou, Y. M. Cr(VI) removal on fungal biomass of *Neurospora crassa*: the importance of dissolved organic carbons derived from the biomass to Cr(VI) reduction. *Environ. Sci. Technol.* **2010**, 44, 6202–6208.
- (40) Molokwane, P. E.; Meli, K. C.; Nkhalambayausi-Chirwa, E. M. Chromium (VI) reduction in activated sludge bacteria exposed to high chromium loading: Brits culture (South Africa). *Water Res.* **2008**, 42, 4538–4548.
- (41) Min, X.; Yuan, C.; Liang, Y.; Chai, L.; Ke, Y. Metal recovery from sludge through the combination of hydrothermal sulfidation and flotation. *Procedia Environ. Sci.* **2012**, *16*, 401–408.
- (42) Watling, H. R. Chalcopyrite hydrometallurgy at atmospheric pressure: 1. Review of acidic sulfate, sulfate—chloride and sulfate—nitrate process options. *Hydrometallurgy* **2013**, *140*, 163–180.
- (43) Wei, Z.; Xiao, S.; Chen, M.; Lu, M.; Liu, Y. Selective oxidation of 5-hydroxymethylfurfural to 2,5-diformylfuran over a Cuacetonitrile complex. *New J. Chem.* **2019**, 43, 7600–7605.
- (44) Pham, A. N.; Rose, A. L.; Waite, T. D. Kinetics of Cu(II) reduction by natural organic matter. *J. Phys. Chem. A* **2012**, *116*, 6590–6599.
- (45) Xing, G.; Garg, S.; Miller, C. J.; Pham, A. N.; Waite, T. D. Effect of chloride and suwannee river fulvic acid on Cu speciation: implications to Cu redox transformations in simulated natural waters. *Environ. Sci. Technol.* **2020**, *54*, 2334–2343.
- (46) Li; Yan, Z. F.; Lu, G. Q.; Zhu, Z. H. Synthesis and structure characterization of chromium oxide prepared by solid thermal decomposition reaction. *J. Phys. Chem. B* **2006**, *110*, 178–183.
- (47) Eriksson, J. Concentrations of 61 trace elements in sewage sludge, farmyard manure, mineral fertiliser, precipitation and in oil and crops; Swedish Environmental Protection Agency Stockholm: 2001; Vol. 5159.
- (48) Arai, S.; Akizawa, N. Precipitation and dissolution of chromite by hydrothermal solutions in the Oman ophiolite: New behavior of Cr and chromite. *Am. Mineral.* **2014**, *99*, 28.
- (49) Eskelsen, J. R.; Xu, J.; Chiu, M.; Moon, J.-W.; Wilkins, B.; Graham, D. E.; Gu, B.; Pierce, E. M. Influence of structural defects on biomineralized ZnS nanoparticle dissolution: an in-situ electron microscopy study. *Environ. Sci. Technol.* **2018**, *52*, 1139–1149.
- (50) Xu, J.; Murayama, M.; Roco, C. M.; Veeramani, H.; Michel, F. M.; Rimstidt, J. D.; Winkler, C.; Hochella, M. F., Jr. Highly-defective nanocrystals of ZnS formed via dissimilatory bacterial sulfate reduction: A comparative study with their abiogenic analogues. *Geochim. Cosmochim. Acta* **2016**, *180*, 1–14.
- (51) Somasundaran, P.; Wang, D., Chapter 3 Mineral—solution equilibria. In *Developments in Mineral Processing*; Wang, D., Ed.; Elsevier: 2006; Vol. 17, pp. 45–72, DOI: 10.1016/S0167-4528(06) 17003-9.

- (52) Hayes, T.; Jewell, W.; Kabrick, R. Heavy Metal Removal from Sludges Using Combined Biological/Chemical Treatment. In *Proc.* (34th) Purdue Ind. Waste Conf., Purdue University, West Lafayette, Indiana, 1980; 1980; pp. 529–543.
- (53) Hayes, T. D.; Theis, T. L. The distribution of heavy metals in anaerobic digestion. J. Water Pollut. Control Fed. 1978, 50, 61–72.
- (54) Ehrlich, H. L. 11 Interactions between microorganisms and minerals under anaerobic conditions. In *Interactions between Soil Particles and Microorganisms: Impact on the Terrestrial Ecosystem*; John Wiley & Sons: 2002; Vol. 7, p 459.
- (55) Yang, Z.; Du, M.; Jiang, J. Reducing capacities and redox potentials of humic substances extracted from sewage sludge. *Chemosphere* **2016**, 144, 902–908.
- (56) Lombi, E.; Donner, E.; Tavakkoli, E.; Turney, T. W.; Naidu, R.; Miller, B. W.; Scheckel, K. G. Fate of zinc oxide nanoparticles during anaerobic digestion of wastewater and post-treatment processing of sewage sludge. *Environ. Sci. Technol.* **2012**, *46*, 9089–9096.
- (57) Wielinski, J.; Gogos, A.; Voegelin, A.; Müller, C.; Morgenroth, E.; Kaegi, R. Transformation of nanoscale and ionic Cu and Zn during the incineration of digested sewage sludge (biosolids). *Environ. Sci. Technol.* **2019**, 53, 11704–11713.
- (58) Zhang, H.; Chen, B.; Banfield, J. F. Particle size and pH effects on nanoparticle dissolution. *J. Phys. Chem. C* **2010**, *114*, 14876–14884.
- (59) Daskalakis, K. D.; George, R. H. The solubility of sphalerite (ZnS) in sulfidic solutions at 25°C and 1 atm pressure. *Geochim. Cosmochim. Acta* **1993**, 57, 4923–4931.
- (60) Hayashi, K.; Sugaki, A.; Kitakaze, A. Solubility of sphalerite in aqueous sulfide solutions at temperatures between 25 and 240°C. *Geochim. Cosmochim. Acta* 1990, 54, 715–725.
- (61) Wei, Z.; Kierans, M.; Gadd, G. M. A model sheet mineral system to study fungal bioweathering of mica. *Geomicrobiol. J.* **2012**, 29, 323–331.
- (62) Ivarsson, M.; Skogby, H.; Phichaikamjornwut, B.; Bengtson, S.; Siljeström, S.; Ounchanum, P.; Boonsoong, A.; Kruachanta, M.; Marone, F.; Belivanova, V.; Holmström, S. Intricate tunnels in garnets from soils and river sediments in Thailand Possible endolithic microborings. *PLoS One* **2018**, *13*, No. e0200351.
- (63) Ivarsson, M.; Broman, C.; Holm, N. G. Chromite oxidation by manganese oxides in subseafloor basalts and the presence of putative fossilized microorganisms. *Geochem. Trans.* **2011**, *12*, 5.
- (64) Oze, C.; Bird, D. K.; Fendorf, S. Genesis of hexavalent chromium from natural sources in soil and groundwater. *Proc. Natl. Acad. Sci. U. S. A.* **2007**, *104*, 6544–6549.
- (65) Kožuh, N.; Štupar, J.; Gorenc, B. Reduction and oxidation processes of chromium in soils. *Environ. Sci. Technol.* **2000**, 34, 112–119.
- (66) Rajapaksha, A. U.; Vithanage, M.; Ok, Y. S.; Oze, C. Cr(VI) formation related to Cr(III)-muscovite and birnessite interactions in ultramafic environments. *Environ. Sci. Technol.* **2013**, *47*, 9722–9729.
- (67) Donner, E.; Ryan, C. G.; Howard, D. L.; Zarcinas, B.; Scheckel, K. G.; McGrath, S. P.; de Jonge, M. D.; Paterson, D.; Naidu, R.; Lombi, E. A multi-technique investigation of copper and zinc distribution, speciation and potential bioavailability in biosolids. *Environ. Pollut.* **2012**, *166*, 57–64.
- (68) Scheinost, A. C.; Kretzschmar, R.; Pfister, S.; Roberts, D. R. Combining selective sequential extractions, X-ray absorption spectroscopy, and principal component analysis for quantitative Zinc speciation in soil. *Environ. Sci. Technol.* **2002**, *36*, 5021–5028.
- (69) Rodgers, K.; Hursthouse, A.; Cuthbert, S. The potential of sequential extraction in the characterisation and management of wastes from steel processing: a prospective review. *Int. J. Environ. Res. Public Health* **2015**, *12*, 11724–11755.
- (70) Bacon, J. R.; Davidson, C. M. Is there a future for sequential chemical extraction? *Analyst* **2008**, *133*, 25–46.
- (71) Apte, A. D.; Tare, V.; Bose, P. Extent of oxidation of Cr(III) to Cr(VI) under various conditions pertaining to natural environment. *J. Hazard. Mater.* **2006**, *128*, 164–174.